

## Solubility of Organic Compounds in Water/Octanol Systems. A Expanded Ensemble Molecular Dynamics Simulation Study of log *P* Parameters

Alexander P. Lyubartsev,<sup>†,\*</sup> Sven P. Jacobsson,<sup>‡,\*</sup> Göran Sundholm,<sup>‡</sup> and Aatto Laaksonen<sup>†</sup>

*Division of Physical Chemistry, Arrhenius Laboratory, Stockholm University, S-106 91, Stockholm, Sweden, and AstraZeneca, Pharmaceutical and Analytical R&D, S-151 85 Södertälje, Sweden*

The expanded ensemble method, developed to calculate solvation free energies, is applied to calculate octanol/water partition coefficients *P* for some organic drug-related molecules and compared with experimental results. The experimental log *P* results were obtained by a miniaturized vial procedure using liquid chromatography with UV for quantification. The expanded ensemble technique, implemented within molecular dynamics scheme, is adapted to treat molecules of arbitrary size and type. For octanol, both all-atom and united atom models are evaluated. The solvation free energy of the organic solute molecules is found to be sensitive to the used sets of partial charges on the atoms in polar groups, particularly in water but also in the saturated octanol phase. Although this effect partially cancels out in the calculated partition coefficients, the charges obtained from ab initio Mulliken population analysis give consistently larger log *P* values than those obtained in simulations with the larger empirical atomic charges included in the CHARMM force field. In general, calculated log *P* turned out to be systematically higher than those measured experimentally. The possibility of improving potential models for the solutes in water and oil phase, respectively, is discussed.

### Introduction

Partition coefficients have a history more than a century long as a measure of how chemical substances become dispersed in living systems and their ability to penetrate into biological boundaries.<sup>1</sup> A transport across biological membranes is of particular importance in pharmacological studies, since it gives information about the absorption, distribution, and elimination of drugs in living organisms.

Selected oil–water systems are commonly used in drug development to investigate the partitioning phenomenon and to calculate the ratio of solubilities of the drug in the aqueous and organic phases. Mixed oil–water phases are also frequently used to extract drugs from plants. Of all oil–water mixtures, the already five-decades-old proposed octanol–water system still holds a strong position and appears to mimic best the behavior of membranes in aqueous solutions, giving reliable measures of possible bioconcentration of drug compounds in tissues. The logarithm of the unitless partition coefficient, log *P*, of a solute between octanol and water is therefore widely applicable in problems like permeability and passive transport through membranes but also in studies of binding to proteins and specific binding at active sites in enzymes.<sup>1–4</sup>

Since a rigorous theoretical determination of log *P*s is a tedious process, many empirical techniques for their calculation have been developed, particularly during the past few decades.<sup>1,2</sup> The total number of published papers aiming at to model and rationalize a general log *P* model can be counted in hundreds, and the applications of log *P* can be found in most diverse fields of bio- and environmental sciences (for some ideas, see for example ref 5). One important use of log *P* include characterizing the properties of the blood–brain barrier.<sup>3,6</sup>

log *P* values, with various modifications of Hammett equations, furnished with empirical steric, hydrophobicity parameters,

or electronic parameters, calculated at some low-level quantum theory, provide a basis to a large amount of quantitative structure–activity relationships (QSAR).<sup>1,4</sup> Also, lipophilicity and permeability data measured by log *P* are used in QSAR.<sup>7,8</sup> Both the additive fragment-based techniques are common approaches,<sup>9</sup> as well as a newer addition method for the log *P* of peptides to be used as a hydrophobicity scale for amino acids<sup>10</sup> and as models estimating the spatial molecular structure to reduce the number of parameters to predict log *P*.<sup>11,12</sup> Further, an intermolecular interaction model inherently including the entropy and solvation effects from experimental log *P* solubilities is developed,<sup>13</sup> and H-bond donor/acceptor descriptors are used for the correlation with permeability.<sup>14,15</sup> A detailed self-consistent-field model for studying complex molecules in inhomogeneous systems, in which all the molecules are represented in a detailed united atom description, is recently suggested where log *P* data are used to give an accurate prediction of the affinity of complex molecules for lipid membranes.<sup>16</sup> Also, we could mention an algorithm for computing the log *P* of conformationally flexible molecules<sup>17</sup> as well as a method for estimating log *P* values derived from three-dimensional molecular structures.<sup>18</sup> From training sets of chemicals, a back-propagation neural network (BNN) model has been developed for calculating log *P*,<sup>19–22</sup> recently released as a software.<sup>23</sup> A number of low-level quantum mechanical calculations are reported to correlate some electronic properties and effective molecular volumes of the solutes to their log *P* values. MNDO-PM3 semiempirical SCF methods showed that the log *P* values were satisfactorily expressed by the van der Waals volume, the total number of hydrogen bonding sites, and the LUMO energy.<sup>24</sup> Differences between the *n*-octanol/water and membrane/water partition coefficients are explored using a small selection of at the AM1 level calculated descriptors.<sup>25</sup> A larger number of molecules of various types and sizes with biological activity, the log *P*s can be represented quantitatively in terms of the solute's molecular surface area, in conjunction with

\* Corresponding authors.

<sup>†</sup> Stockholm University.

<sup>‡</sup> AstraZeneca.

statistically based quantities calculated from its surface electrostatic potential at the STO-3G\*/STO-5G\*<sup>26</sup> and HF/6-31G\* levels of HF theory.<sup>27</sup> For an overview of the methods used to calculate  $\log P$ , the reader is referred to several excellent reviews in recent literature.<sup>1–4</sup>

In this context, a few previous related computer simulations or computer calculations of  $\log P$ s should be mentioned. The free energy perturbation (FEP) method, implemented within the MD framework was used to calculate differences in  $\log P$ s.<sup>28</sup> The partition coefficient of cyclosporin A (CsA) was measured in octanol/water and heptane/water. MD simulations in water and CCl<sub>4</sub> support the suggestion that CsA undergoes solvent-dependent conformational changes.<sup>29</sup> MD simulations were also carried out to analyze octanol/water solvation-shell structuring around the solutes to gain insight into hydrated 1-octanol's capability to serve as a biophase analog.<sup>30</sup> Monte Carlo (MC) simulations were performed for the  $\log P$ ,<sup>31</sup> and a continuum Poisson–Boltzmann hydration model has been extended to the octanol–water transfer.<sup>32</sup> A general stochastic algorithm based on the simulated annealing method was applied to search for structures having low  $\log P$ .<sup>33</sup> MD free energy perturbation (FEP) simulations were carried out to estimate the relative  $\log P$  and compared to GB/SA octanol continuum solvation model<sup>34</sup>. Chen and Siepmann have used Gibbs ensemble Monte Carlo simulations to calculate partitioning of short alkanes and alcohols between water, octanol, and a gas phase.<sup>35</sup> Also, computer simulations of other partition coefficients than  $\log P$ s have been reported.<sup>36–41</sup>

In this work, we report calculations of  $\log P$  parameters for a selected set of drug related compounds on the basis of solvation free energy simulations by means of the expanded ensemble (EE) method<sup>42</sup> within the frame of molecular dynamics (MD) computer simulations.<sup>43</sup> The EE method provides a rigorous and accurate way of modeling the two phase system at specific physical conditions, including effects from temperature, entropy, and environment, with varying concentration.

This paper is organized as follows: the next section gives the experimental details in measurements of the  $\log P$  values. The Computational Details section gives a short review of the expanded ensemble method used to calculate the absolute solvation free energies. Also, the computational details concerning the MD simulation scheme and the force field models are given. Then the Results and discussion section follows, starting with an evaluation of the molecular models used for the octanol phase. Results from calculations of solvation structure around the solutes, solvation free energies, and the partition coefficients are discussed in details. Finally, the conclusions are given in the end of the paper.

## Experimental Section

**Instrumentation.** The primary apparatus is a Hewlett-Packard HP3D 1100 LC system with a diode-array detector. The chromatographic separation is performed at pH 7.4 (TRIS-buffer,  $I = 0.01$ ) on a Waters SymmetryShield RP-8 column using a fast gradient from 5 to 90% acetonitrile in 5 min. The detection is at 210 nm.

**$\log P$  Determination.** The general procedure is described in ref 44. Typically, about 2 mg of the compound is wetted with 10  $\mu$ L of DMSO and then dissolved in 500  $\mu$ L of octanol in a 1000  $\mu$ L tapered LC-vial (the amount of DMSO was found not to have any practical influence on the magnitude of the measured value). Then 500  $\mu$ L of 0.15 mol L<sup>-1</sup> of NaOH is added. The vial is capped, and the mixture is agitated for at least 20 min at ambient temperature (22 °C), depending on the lipophilicity of

the compound. After centrifugation, 1 aliquot of the octanol phase is transferred to another vial and diluted up to 100 times, depending on the theoretically estimated  $\log P$ . The rest of the octanol phase is discarded, leaving the water phase in the vial for subsequent quantification. Thereby, transfer of the aqueous phase to another vial is avoided and possible adsorption losses minimized. This phase separation and dilution procedure is automated using a Gilson 221 autosampler. The amounts of the amine in the phases are quantified using the fast gradient LC method with UV-detection. Between 1 and 100  $\mu$ L of the samples is injected, depending on the theoretically estimated  $\log P$ .

## Computational Details and Molecular Models

**Expanded Ensemble Method.** The  $\log P$  partition coefficient can be directly related to the difference of solvation free energy in water and octanol phase, respectively

$$\log P = \frac{1}{2.303RT}(G_{\text{water}} - G_{\text{oct}}) \quad (1)$$

where  $G_{\text{water}}$  and  $G_{\text{oct}}$  are the solvation free energies of the solute substance in water and octanol, correspondingly. The expanded ensemble (EE) method for solvation free energy calculations was originally developed within Monte Carlo methodology<sup>42</sup> and later modified for molecular dynamics simulation techniques.<sup>43</sup> In comparison with other methods, the EE scheme has shown to be both highly efficient and accurate. While most other methods need a series of repeated computer simulation runs to obtain the free energy value, using the EE method, only one single run is required after a proper choice of a set of the transition parameters (balancing factors) which can be easily determined in a few short trial runs. Full details of the EE method can be found in the original papers.<sup>42,43</sup> The method has been used by us mainly on small solutes, such as ions and methane dissolved in water,<sup>45,46</sup> but applications to polymer models<sup>47,48</sup> or to molecules like benzene and cyclohexane<sup>49–51</sup> have been reported. This current work is our first application of the EE method to the areas of arbitrarily large, flexible solutes.

Using the EE method implies a gradual insertion/deletion of the studied solute particle into/from the solvent. The insertion parameter  $\alpha$  is introduced, which is a scaling factor for the part of the Hamiltonian, describing the interaction of the solute particle with the solvent. The case  $\alpha = 0$  corresponds to the pure bulk solvent, while the case  $\alpha = 1$  corresponds to the fully inserted solute particle. The insertion parameter is considered as a configurational space variable and will change during the simulation according to the Monte Carlo rules for the canonical ensemble defined by the configurational partition function

$$Z = \sum_{m=0}^M \int \prod_{i=1}^{N+1} dr_i \exp\{-\beta[H_N(r_i) + H_{\text{int}}(r_{N+1}) + \alpha_m h_{N+1}(r_i)] + \eta_m\} \quad (2)$$

where  $\beta = 1/kT$ ,  $H_N$  is the potential energy of  $N$  solvent particles,  $H_{\text{int}}$  is the intramolecular potential energy of the solute,  $h_{N+1}$  is the potential energy of interaction of  $N + 1$ -th (solute) particle with all other solvent particles,  $\alpha_m$ 's are numbers changing from 0–1 while  $m$  changes from 0– $M$  (insertion parameter), and  $\eta_m$ 's are balancing factors, or biased potentials, which are introduced in order to facilitate changes of the insertion parameter. A Monte Carlo random walk in the expanded space of  $\{r_i\}$  and  $m$ , consisting of displacements of the both particles and changes

of  $m$ , produces a probability distribution over the sub-ensembles  $p_m$ . The excess solvation (Helmholtz) free energy can be determined from the probability ratio of the two extreme subensembles<sup>46</sup>:

$$\beta F_{\text{solv}} = -\ln \frac{p_M}{p_0} + \eta_M - h_0 \quad (3)$$

The Gibbs free energy  $G$  can be obtained by applying the same scheme in the constant-pressure ensemble<sup>45</sup>. The balancing factors  $\eta_m$  must be chosen in a way to provide “measurable” (in a finite MC run) probabilities  $p_m$ . They can be tuned in a few short trial runs. If the probabilities of some subensembles are too low (or zero) in a trial run, one should increase the  $\eta_m$  parameters for these points. Also, the  $\alpha_m$  points must be chosen close enough to each other in order to provide a reasonably high transition probability between the sub-ensembles. The strategy of choosing  $\alpha_m$  and  $\eta_m$  parameters is discussed in details in our previous papers.<sup>42,45</sup>

**Water and Octanol Phases.** As the solvent water model, we have used the flexible SPC potential by Toukan and Rahman<sup>52</sup>. In this model, the stretching of the O–H bond is made anharmonic by means of a Morse potential. The Toukan–Rahman model gives both the dielectric constant and diffusion coefficient in good agreement with experiments<sup>53</sup>. Two models for octanol have been evaluated. In the first model (UA), the hydrocarbon groups ( $\text{CH}_2$ ) and ( $\text{CH}_3$ ) treated using the united atom approach by describing them as single Lennard–Jones spheres. The potential model parameters are adopted from<sup>30</sup>. Another all-atomic model (AA) was constructed and based on the CHARMM force field<sup>54</sup>. In this second model, the Morse potential is used for stretching of the O–H bond in order to better match with the used water model<sup>52</sup> which also contains the same type of anharmonic stretching modes for O–H bonds.

**Modeling the Solutes.** Four drug-related compounds, benzylamine, phenylethylamine, lidocaine, and ebalzotan (see Figure 1a–d), have been studied. Molecular models for solute molecules have been constructed on the basis of the CHARMM22 force field<sup>54</sup> by looking through the database for proteins and lipids for similar molecular fragments to prescribe the parameters for the simulated solute molecules. For the first two molecules, two sets of atomic charges have been tested: one is taken from similar molecular fragments in the CHARMM force field; the other is taken from the Mulliken population analysis, carried out in quantum chemical calculations, is performed with the density functional theory (DFT) at the B3LYP/6-311G(d,p) level using the Gaussian 98<sup>55</sup> program package. The atomic charges, used in the simulation, are given in Figure 1, as well as the atomic types according to the CHARMM notation. As a rule, the DFT charges are somewhat smaller than the corresponding CHARMM charges. This is a consequence of the fact that the quantum chemical DFT charges were calculated in a vacuum, while CHARMM charges are empirically fitted for simulations in aqueous solution conditions.

For each solute molecule, preceding vacuum MD simulations were carried out to ensure that the force field reproduces the quantum chemically optimized geometries, whereby a satisfactory agreement was found.

**Simulation Details.** The MD simulations<sup>56,57</sup> were carried out in the NPT ensemble by coupling the temperature and pressure to separate N  se–Hoover<sup>58,59</sup> thermostats and barostats, respectively. The multiple time step method by Tuckerman et al.<sup>60</sup> was employed to integrate the equations of motion. For the fast molecular motions, e.g., bond stretching, angle bending,

motion of torsional and improper torsional angles, and nearest-neighbor nonbonded interactions, a time step of 0.2 fs was used, while for the long-range nonbonded interactions, the time step was set to 2 fs. The Ewald summation has been applied to treat the electrostatic interactions.

In all simulations, the temperature was set to 298 K and the pressure to 1 atm. Calculations of the solvation free energy in the water phase have been performed for one solvent molecule dissolved in 255 water molecules. Simulations of the oil phase have been done for one solute molecule, 64 octanol molecules, and 24 water molecules. The latter case corresponds to the experimental value of 27% molar ratio of water in a saturated water/octanol mixture. We should note that in the model mixture presented by the SPC/OPLS or SPC/CHARMM potentials, the saturation ratio may be different than what was observed in ref 35. However, we chose to fix the water/octanol fraction equal to the experimental value in order to mimic possibly better the experimental conditions. The size of our system is small enough that allows us to avoid undesirable effects (e.g., phase separation) due to possible thermodynamical instability.

The insertion parameter  $\alpha$  in the EE method was varied from 0 to 1 in 30 steps for the first two, smaller solutes and in 35 and 40 steps for the much bigger lidocaine and ebalzotan. The  $\alpha$ -points have been chosen to be more condensed close to zero because the effective diameter of the Lennard–Jones potential decreases very slowly upon decreasing of the insertion parameter. The balancing factors  $\eta_m$  for the EE run for the benzylamine molecule have been obtained in five trial runs with a total simulation time about 200 ps. It turned out that the same balancing factors may be (and have been) used for phenylethylamine because this molecule is similar to benzylamine. This choice of balancing factors allows the system to walk between the states with fully inserted and completely free solute during a time of about 30–50 ps, thus providing a reasonable distribution over the insertion parameter, and hence the free energy, after a few hundred picoseconds of simulation. An example of reasonable optimized  $\alpha_m$  and  $\eta_m$  parameters, as well as calculated probability distribution and free energies, for the case of solvation of phenylethylamine molecule in water are given in Table 1. The dependence of optimized  $\eta_m$  parameters on the insertion parameter  $\alpha$  in other cases follows the same pattern: first, rapid growth of  $\eta_m$  with  $\alpha_m$ , corresponding to positive free energy change to create a cavity in the solvent. Then, when parameter  $\alpha$  is approaching to 1, the attractive part of the interaction plays a more important role, and optimized  $\eta_m$ , as well as free energies, decreases, eventually becoming negative.

For the two smaller solutes, actual simulation time in this work was 1 ns, which provides the precision of about 1 kJ/M for the solvation free energy. Finding the optimal balancing factors for lidocaine, and especially for ebalzotan, turned out to be more intricate than for the smaller molecules. A simulation of almost 1 ns had to be spent for this purpose. Thereafter, a 5 ns simulation was performed for lidocaine and 10 ns for ebalzotan to calculate the final value of the solvation free energy with a precision of 2 kJ/M.

The computations were carried out using a modified version of the general purpose computer simulation package for arbitrary mixtures, **MDynaMix**, by Lyubartsev and Laaksonen<sup>61</sup>, implementing the expanded ensemble method into the code. The simulation have been carried out on an Intel PC running Linux as the operating system.

## Results and Discussion

**Simulations of Octanol Phase.** To evaluate the used octanol models, test simulations were carried out of pure octanol phase.

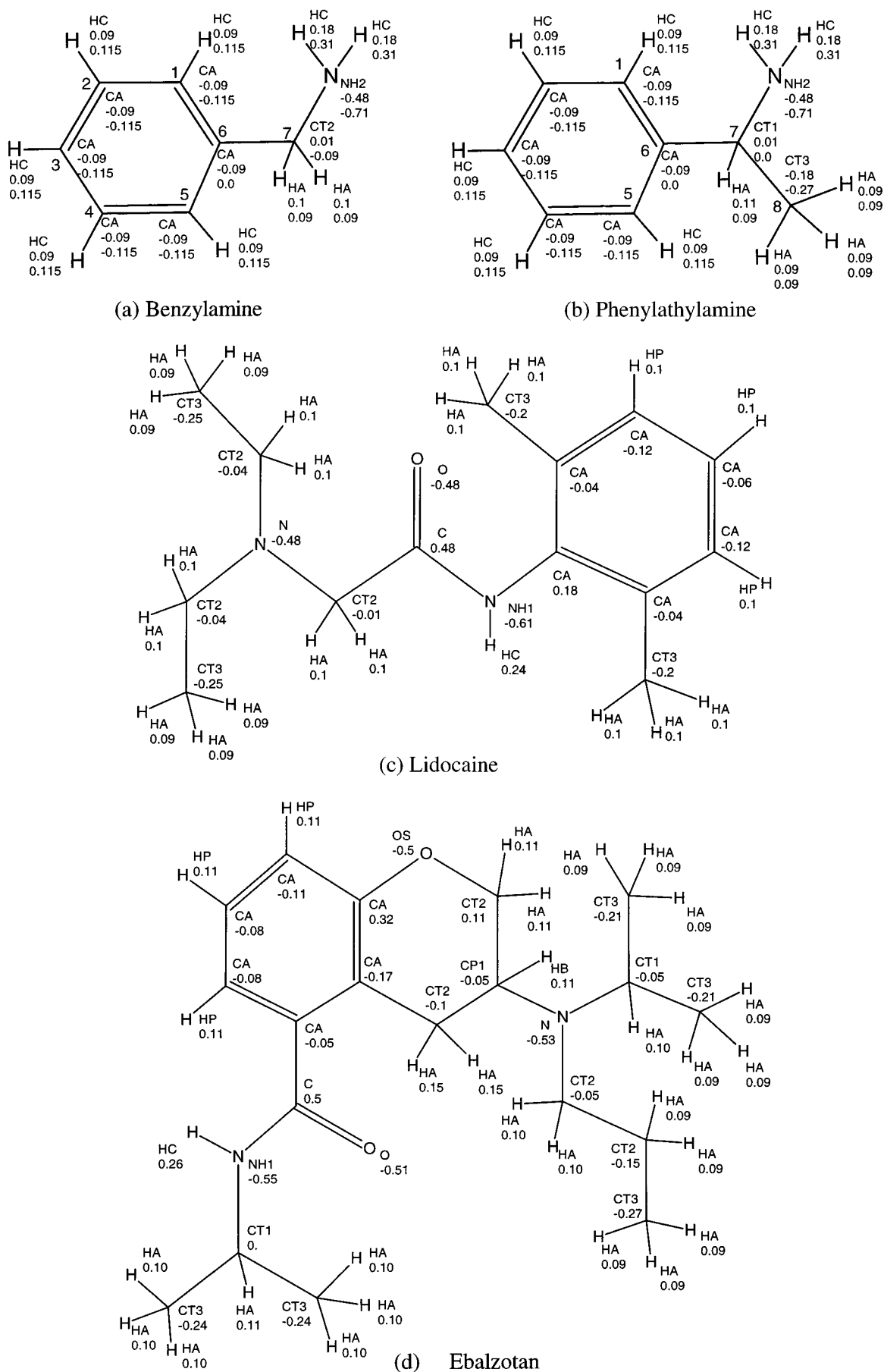


Figure 1. Molecular structures of drug molecules, studied in this work



**TABLE 1: Example of an EE Simulation Protocol for Calculation of Solvation Free Energy of Phenylethylamine in Water<sup>a</sup>**

<i>m</i>	$\alpha_m$	$\eta_m$	$p_m$	$G_{\text{solv}}$ (kT)	$G_{\text{solv}}$ (kJ/M)
0	0.0	0.0	0.012 46	0.0	0.0
1	$2 \cdot 10^{-7}$	1.9	0.013 48	1.824	4.550
2	$10^{-6}$	2.8	0.013 44	2.7241	6.7948
3	$3 \cdot 10^{-6}$	3.7	0.014 06	3.5789	8.9268
4	0.000 01	4.9	0.014 21	4.7683	11.8935
5	0.000 03	6.3	0.012 50	6.2970	15.7066
6	0.0001	8.3	0.011 85	8.3500	20.8273
7	0.0002	9.6	0.012 39	9.6054	23.9588
8	0.0005	11.3	0.011 18	11.4086	28.4564
9	0.001	12.6	0.009 06	12.9191	32.2240
10	0.002	14.5	0.013 67	14.4075	35.9367
11	0.003	15.6	0.017 47	15.2617	38.0673
12	0.005	16.7	0.019 45	16.2544	40.5434
13	0.007	17.3	0.017 85	16.9405	42.2547
14	0.01	17.9	0.016 32	17.6301	43.9747
15	0.015	18.8	0.018 66	18.3961	45.8855
16	0.02	19.6	0.024 14	18.9386	47.2386
17	0.03	20.6	0.031 42	19.6751	49.0755
18	0.06	21.8	0.041 05	20.6076	51.4016
19	0.1	22.4	0.059 83	20.8310	51.9586
20	0.15	22.7	0.107 09	20.5487	51.2547
21	0.2	21.9	0.091 96	19.9011	49.6393
22	0.3	19.3	0.046 40	17.9851	44.8602
23	0.4	16.7	0.040 24	15.5276	38.7304
24	0.5	14.1	0.047 44	12.7629	31.8344
25	0.6	11.2	0.056 02	9.6967	24.1865
26	0.7	7.7	0.047 04	6.3714	15.8923
27	0.8	4.2	0.053 71	2.7388	6.8314
28	0.9	0.3	0.057 34	-1.2266	-3.0594
29	1.0	-3.8	0.068 32	-5.5018	-13.7231

<sup>a</sup> Atom types according to CHARMM22 nomenclature; DFT charges and charges adopted from the CHARMM force field are shown for each atom.

**TABLE 2: Some Physical Properties of the Used Octanol Models at  $T = 298$  K and  $P = 1$  atm**

model	UA	AA	exp
density (g/cm <sup>3</sup> )	0.816(5)	0.808(5)	0.827
$\Delta H_{\text{vap}}$ (kJ/M)	68.0(0.5)	64.5(0.5)	65.3

The results on the evaporation energy  $\Delta H_{\text{vap}}$  and density (corresponding to pressure 1 atm) are given in Table 2, in comparison with experimental data. Evaporation energy is evaluated from the difference of total energy per molecule in the gas phase (isolated molecule) and in the liquid. For the united atom octanol model, our results agree well with the results of work.<sup>30</sup> It can be seen that the united atom model provides a better agreement with experimental data for the density, while the all-atom model provides a better evaporation energy. Still, in both cases, the agreement is satisfactory.

**Solvation Free Energies and log  $P$ .** The simulation results for the solvation free energy are shown in Table 3 and for partition coefficients in Table 4. The statistical uncertainty was estimated from the variance of the intermediate values obtained by averaging over smaller pieces of the MD trajectories and was found to be about  $\pm 1$  kJ/M for benzylamine and phenylethylamine and  $\pm 2$  kJ/M for lidocaine and ebalzotan. Correspondingly, for the partition coefficients, we have uncertainty 0.2 for the two smaller molecules and 0.4 for lidocaine and ebalzotan.

One of the problem of simulation of saturated water/octanol solution is possibility of formation of microclusters, or inverse micelles, consisting of octanol polar groups and water molecules.<sup>30,34</sup> In our simulations, we observed typically 1–2 such microclusters in each configuration. They were of the same size

**TABLE 3: Summary of Results for Solvation Free Energies (in kJ/M)<sup>a</sup>**

molecule	$G_{\text{water}}$	$G_{\text{octanol}}$	$G_{\text{octanol}}$
		UA	AA
benzylamine <sup>b</sup>	-12.5	-24.5	-22.1
benzylamine <sup>c</sup>	-7.8	-22.7	-20.8
phenylethylamine <sup>b</sup>	-13.4	-24.6	-24.0
phenylethylamine <sup>c</sup>	-8.5	-21.8	-21.2
lidocaine	-34	-53	
ebalzotan	-44	-70	

<sup>a</sup> AA and UA denote all-atom and united atom octanol models, respectively. <sup>b</sup> Atomic charges taken from the CHARMM force field. <sup>c</sup> Mulliken charges from DFT calculations. See text for details.

(10–20 water molecules and octanol polar groups) as those in the work of DeBolt and Kollman.<sup>30</sup> Such microclusters may pose certain problems for simulations because they may exist quite a long time and then dissolve and form aggregates of another structure. To check stability of our calculations with respect to possible reorganization of octanol–water structure, we have performed several test calculations for benzylamine and phenylethylamine in octanol phase differing by initial conditions, generated by separate high-temperature runs. The results (a serie of four independent runs of 1 ns) differ from the average value (shown in Table 2) by no more than 1.2 kJ/M, providing about the same variance as averaging over different pieces of the same trajectory. It was noted earlier that the expanded ensemble method appears to be very useful in treating the “multiple minima problem”.<sup>42,62</sup> In the present case of solvation free energies, when parameter  $\alpha$  becomes zero, the solute particle moves freely inside the solvent, appearing afterward (when  $\alpha$  begin increase) in another place, thus sampling efficiently during a single run both octanol-rich and polar-group-rich regions in the simulation cell.

Comparison of the calculated and experimental results shows that the simulated partition coefficients become systematically overestimated. Similar observation have been made in ref 35 for some alcohol solutes simulated by the OPLS parameter set. Naturally, the results depend directly on the chosen molecular model. We found that the choice of partial atomic charges has a significant influence on the obtained results. The set of charges, taken from the CHARMM force field are only slightly larger in magnitude than the Mulliken charges, obtained from our DFT calculations, except for the atoms of the amino group, where the difference is more significant. However, this difference exerts a strong influence on the solvation free energy in water phase. This can, of course, be expected due to the fact that an increase of the partial charges will enhance the hydrophilic character of the amino group, leading to a more negative solvation free energy in water. At the same time, the solvation free energies in the oil phase are less affected by the choice of charges. As a result, an increase of the magnitudes of the charges of the polar groups leads consequently to lower partition coefficients and, in our case, to a better agreement with the experiment.

For lidocaine and ebalzotan, we have only used the obtained set of atomic Mulliken charges in the DFT calculations. The reason is that the CHARMM database did not contain all the needed fragments of these molecules. Using a renormalized “solvent-polarized” set of atomic charges should improve the result for these two much larger molecules.

It is a standard procedure to calculate the atomic charges in quantum calculations on the basis of either Mulliken population analysis or various schemes to obtain the electrostatic potentials. All these calculations are carried out in vacuum conditions.

**TABLE 4: Comparison of Calculated and Experimental Partition Coefficients<sup>a</sup>**

solute	model	log $P_{\text{calc}}$	log $P_{\text{exp}}$	ACD <sup>d</sup>	hyperChem <sup>e</sup>	pallas <sup>f</sup>
benzylamine	AA <sup>b</sup>	1.7 ± 0.2	0.97	1.09	1.16	1.07
	AA <sup>c</sup>	2.1 ± 0.2	1.09 <sup>g</sup>			
	UA <sup>b</sup>	2.1 ± 0.2				
	UA <sup>c</sup>	2.5 ± 0.2				
phenylethylamine	AA <sup>b</sup>	1.8 ± 0.2	1.31	1.44	1.42	1.50
	AA <sup>c</sup>	2.2 ± 0.2				
	UA <sup>b</sup>	1.9 ± 0.2				
	UA <sup>c</sup>	2.3 ± 0.2				
lidocaine	UA <sup>c</sup>	3.3 ± 0.4	2.26	2.36	2.39	2.78
ebalzotan	UA <sup>c</sup>	4.5 ± 0.4	3.27	3.76	3.56	3.83

<sup>a</sup> AA and UA denote all-atom and united atom octanol models, respectively. Two sets of atomic charges are used in the simulations. Added in the table are results calculated using a few log  $P$  calculator software. <sup>b</sup> Atomic charges taken from the CHARMM force field. <sup>c</sup> Mulliken charges from DFT calculations. See text for details. <sup>d</sup> log  $P$  calculator version 3.5 from Advanced Chemistry Developments Inc., Ontario, Canada. <sup>e</sup> log  $P$  function in HyperChem version 5.0 from Hypercube Inc., Gainesville, FL. <sup>f</sup> The PrologP modules in Pallas version 2.2 from CompuDrug International Inc., San Francisco, CA. <sup>g</sup> Ref 4.

Inclusion of effects of surrounding molecules in liquids and solutions often leads to a polarization and consequently to an increase of atomic charges. The parameters in the CHARMM force field are empirically adjusted to reproduce the molecular behavior in aqueous solution. The larger atomic charges, especially on polar groups, reflect the effect of water as the solvent. It is not clear how applicable the charges are in a much less polar solvent such as octanol, where the effect of the dielectric polarization is smaller than that in water.

Quite interestingly, if we take our results for the solvation free energy calculated using the CHARMM charges in water phase and used the DFT Mulliken charges in oil phase, we obtain partition coefficients  $1.5 \pm 0.2$  for benzylamine in UA and AA octanol model and  $1.5 \pm 0.2$  and  $1.4 \pm 0.2$  for phenylethylamine in UA and AA octanol model. This gives substantially better agreement with the experiment. Intuitively, it does not seem unreasonable to use different partial atomic charges for solute models in very much different solvents with completely different dielectric properties such as the highly polar water and the oily octanol. This is analogous for using different dielectric constants in continuum model or vacuum studies to describe solvent effects. Aspects concerning water- and oil-phase adapted charges will be investigated in more details in our forthcoming paper.

There are several methods to include “solvent” into ab initio quantum chemical calculations. Examples of these include the self-consistent reaction field (SCRF), where the solute molecule is placed in a cavity with a surrounding dielectricum within the Onsager model<sup>63</sup> and the polarized continuum model.<sup>64</sup> It is also possible to run the ab initio calculations by attaching a few water molecules around the solute, preferably in hydrogen bond positions. In addition to the Mulliken population analysis, it is common to calculate electrostatic potential (ESP) fitted charges. Applications of different schemes of charge calculation can yield rather different results for the considered solute molecules. Within the level of theory, used in the present work, the ESP scheme turned out to give unrealistically large negative charges to some of the carbon atoms for both lidocaine and ebazotan. Which is the primary reason for us to use Mulliken charges in this work. Clearly, a reliable enough evaluation of partial atomic charges for larger and flexible molecules in varying solvent environments still remains as a challenging problem in the computational chemistry.

Cieplak has studied the dependence of the solvation free energies on atomic charge distribution using free energy perturbation method in MD simulations of methanol in water.<sup>65</sup> By attaching hypothetical atomic charges on the solute, all giving same total molecular dipole moment, the differences in

hydration free energies were calculated. The center of the charge distribution and the orientation of the total dipole moment within the Lennard–Jones envelope was found to affect the electrostatic contribution to the hydration free energies.

For benzylamine and phenylethylamine, we also carried out calculations of the solvation free energy in octanol phase using an all-atom (AA) octanol model. This yields solvation free energies which are about 1–2 kJ/M less negative than those calculated using the UA octanol model. Correspondingly, the agreement with the experiment is better for the all-atom octanol model. However, inclusion of all the hydrogens in the simulation leads to an almost 3-fold increase of the computer time.

It is also worth to note that, independently on the model used, the calculated partition coefficients closely follow the experimental trends. Both simulations and experimental data provide, within the error limits, similar partition coefficients for benzylamine and phenylethylamine, somewhat greater for lidocaine, and even greater for ebazotan. The systematic error in the calculated partition coefficients can be explained by the necessity to take into account solvent effects on the partial atomic charges.

**log  $P$  Calculators.** In Table 4, are a few examples of log  $P$  values quoted, calculated using some of the log  $P$  calculators found in the commercial software market. The software used are the version 3.5 log  $P$  calculator from Advanced Chemistry Developments Inc., the log  $P$  function in version 5.0 HyperChem from HyperCube Inc., and the prologP modules in version 2.2 Pallas from CompuDrug International Inc..

The ACD log  $P$  calculator contains a database with 3600 structures with 500 different functional groups as well as a possibility to train the system to improve accuracy. The algorithm is based on contributions of separate atoms, structural fragments, and intramolecular interactions between the fragments, derived from the database of structures with reported experimental log  $P$  values. It is claimed to give the values within  $\pm 0.3$  log  $P$  units for most neutral molecules. Using HyperChem, the log  $P$ s are calculated in the ChemPlus suite of auxiliary programs and its QSAR property package. Also, the prologP disintegrates the molecules to fragments, expressing the log  $P$  value as a superposition of corresponding fragment constants. All the three empirical log  $P$  predictors do a reasonable job for the set of molecules studied in this work. One should have in mind, however, that the considered molecules, with a possible exception ebazotan, have been used in the training data sets for the empirical calculators. For molecules not included into training data sets, results may differ significantly. For example, for the case of ebazotan, the difference between experimental value and predictions of the three empirical methods is between 0.4 and 0.6. Using molecular dynamics, even with empirical

force field parameters, is in some sense a more ab initio way of predicting log *P* parameters. Though in the present work we did not reproduce the log *P* values better than the empirical methods, the work on optimization of the force field parameters may result in more reliable prediction of the partition coefficients using free energy calculations in molecular simulations

## Conclusions

Our study clearly shows that our expanded ensemble method provides a realistic way to calculate solvation free energies and the partition coefficients for typical and complex drug structures based on atomistic molecular dynamics simulations. Not only can the relative changes be calculated, as reported recently by Best et al.<sup>34</sup> in their implementation of free energy perturbation method, but the absolute values of partition coefficients can also be calculated. The simulated time, including the time needed for optimizing the balancing parameters of the EE method, varies from 2 ns for molecules like bensylamine (8–10 heavy atoms) to 10 ns for molecules like ebalzotan (20–25 heavy atoms) to provide a computational uncertainty about 0.2 for the partition coefficients. Computer simulations covering tens of nanoseconds are standard today and can be performed now on low-cost modern personal computers. Our study also shows that the choice of molecular model, or the force field, is of crucial importance for the calculation of partition coefficients. This concerns first of all the choice of partial atomic charges. Other parameters of the force field may be also important. For example, this the case for the short-ranged Lennard–Jones parameters of the solutes while penetrating into the oil phase. It has been noticed previously that the solvation free energy calculations are very sensitive to the parameters of molecular models.<sup>46</sup> From this point of view, experimental data related to the solvation free energies could be beneficially used for a fine-tuning of empirical molecular models.

Most of the numerous log *P* and related partition coefficient calculators do a reasonably good job in predicting the hydrophobic and lipophilic parameters. The aim of the present work is not to introduce an alternative computational scheme to do the same. The value of the presented method is mainly 2-fold. First, a systematic investigation of organic solutes in water and octanol phase and calibration of the force field parameters (in particular the atomic charges) against the experimental log *P* values should greatly improve the quality of the potential parameters used in the atomistic computer simulations of solutes in solvents. The second and a natural motivation is to use both the EEMD and conventional MD methods with the optimized molecular models to study organic molecules dissolved in arbitrary systems containing biological barriers, not least in phospholipid bilayer membrane systems because of the excellent correlation between the log *P* values and the permeability and transport in membranes. From pharmacological point of view, we should, for example be able to reveal both unwanted and enhanced effects when other molecules are added along with the drugs. Also, physical conditions can be easily changed during a computer simulations. For example, a weak electric potential across the membrane mimicking the ion distribution.

**Acknowledgment.** This work has been supported by the Swedish Natural Research Council (NFR).

## References and Notes

- (1) Buchwald, P.; Bodor, N. *Curr. Med. Chem.* **1998**, *5*, 353–380.
- (2) Leo, A. J. *Chem. Rev.* **1993**, *93*, 1281–1306.
- (3) Bodor, N.; Buchwald, P. *Adv. Drug Delivery. Rev.* **1999**, *36*, 229–254.
- (4) Leo, A. J.; Hansch, C. *Perspect. Drug Discovery Design* **1999**, *17*, 1–25.
- (5) Matoba, Y.; Yoshimura, J.; Ohnishi, J.; Mikami, N.; Takimoto, Y.; Matsuo, M. *J. Pestic. Sci.* **1999**, *24*, 60–68.
- (6) Gratton, J. A.; Abraham, M. H.; Bradbury, M. W.; Chadha, H. S. *J. Pharm. Pharmacol.* **1997**, *49*, 1211–1216.
- (7) Carpy, A. *Analysis* **1999**, *27*, 3–6.
- (8) Hayashi, M.; Nakamura, Y.; Higashi, K.; Kato, H.; Kishida, F.; Kaneko, H. *Toxicol. Vitro* **1999**, *13*, 915–922.
- (9) Waller, C. L. *Quant. Struct.-Act. Relat.* **1994**, *13*, 172–176.
- (10) Tao, P.; Wang, R. X.; Lai, L. H. *J. Mol. Model.* **1999**, *5*, 189–195.
- (11) Bodor, N.; Buchwald, P. *J. Phys. Chem. B* **1997**, *101*, 3404–3412.
- (12) Buchwald, P.; Bodor, N. *J. Phys. Chem. B* **1998**, *102*, 5715–5726.
- (13) Kellogg, G. E.; Abraham, D. J. *Analysis* **1999**, *27*, 19–23.
- (14) Raevsky, O. A.; Schaper, K. J.; Seydel, J. K. *Quant. Struct.-Act. Relat.* **1995**, *14*, 433–436.
- (15) Raevsky, O. A.; Schaper, K. J. *Eur. J. Med. Chem.* **1998**, *33*, 799–907.
- (16) Meijer, L. A.; Leermakers, F. A. M.; Lyklema, J. *J. Chem. Phys.* **1999**, *110*, 6560–6579.
- (17) Richards, N. G. J.; Williams, P. B.; Tute, M. S. *Int. J. Quantum Chem.* **1992**, *44*, 219–233.
- (18) Sasaki, Y.; Kubodera, H.; Matuszaki, T.; Umeyama, H. *J. Pharmacobio-dyn.* **1991**, *14*, 207–214.
- (19) Breindl, A.; Beck, B.; Clark, T.; Glen, R. C. *J. Mol. Model.* **1997**, *3*, 142–155.
- (20) Schaper, K. J.; Samitier, M. L. R. *Quant. Struct.-Act. Relat.* **1997**, *16*, 224–230.
- (21) Devillers, J.; Domine, D.; Guillon, C.; Karcher, W. *J. Pharm. Sci.* **1998**, *87*, 1086–1090.
- (22) Devillers, J. *SAR QSAR Environ. Res.* **1999**, *10*, 249–262.
- (23) Devillers, J. *Analysis* **1999**, *27*, 23–29.
- (24) Katagi, T.; Miyakado, M.; Takayama, C.; Tanaka, S. *ACS Symp. Ser.* **1995**, *606*, 48–61.
- (25) Vaes, W. H. J.; Ramos, E. U.; Verhaar, H. J. M.; Cramer, C. J.; Hermens, J. L. M. *Chem. Res. Toxicol.* **1998**, *11*, 847–854.
- (26) Brinck, T.; Murray, J. S.; Politzer, P. *J. Org. Chem.* **1993**, *58*, 7070–7073.
- (27) Haeblerlein, M.; Brinck, T. *J. Chem. Soc., Perkin Trans. 2* **1997**, pages 289–294.
- (28) Essex, J. W.; Reynolds, C. A.; Richards, W. G. *J. Am. Chem. Soc.* **1992**, *114*, 3634–3639.
- (29) Eltayyar, N.; Mark, A. E.; Vallat, P.; Brunne, R. M.; Testa, B.; VanGunsteren, W. F. *J. Med. Chem.* **1993**, *36*, 3757–3764.
- (30) Debolt, S. E.; Kollman, P. A. *J. Am. Chem. Soc.* **1995**, *117*, 5316–5340.
- (31) Kuhne, R.; Breitkopf, C.; Schuurmann, G. *Environ. Toxicol. Chem.* **1997**, *16*, 2067–2069.
- (32) Schmidt, A. B.; Fine, R. M. *Biopolymers* **1995**, *36*, 599–605.
- (33) Faulon, J. L. *J. Chem. Inf. Comput. Sci.* **1996**, *36*, 731–740.
- (34) Best, S. A.; Merz, K. M.; Reynolds, C. H. *J. Phys. Chem. B* **1999**, *103*, 714–726.
- (35) Chen, B.; Siepmann, J. I. *J. Am. Chem. Soc.* **2000**, *122*, 6464–6467.
- (36) Auffinger, P.; Wipff, G. *J. Chim. Phys. Phys. Chim. Biol.* **1991**, *88*, 2525–2534.
- (37) Seras, M.; Ollivon, M.; Edwards, K.; Lesieur, S. *Chem. Phys. Lipids* **1993**, *66*, 93–109.
- (38) Sheng, Q.; Schulten, K.; Pidgeon, C. *J. Phys. Chem.* **1995**, *99*, 11018–11027.
- (39) Yang, C. Y.; Cai, S. J.; Liu, H. L.; Pidgeon, C. *Adv. Drug Delivery Rev.* **1997**, *23*, 229–256.
- (40) Boyd, R. H.; Chance, R. R.; Strate, G. V. *Macromolecules* **1996**, *29*, 1182–1190.
- (41) Schurhammer, R.; Wipff, G. *New J. Chem.* **1999**, *23*, 381–391.
- (42) Lyubartsev, A. P.; Martynovskii, A. A.; Shevkunov, S. V.; Vorontsov-Velyaminov, P. N. *J. Chem. Phys.* **1992**, *96*, 1776–1783.
- (43) Lyubartsev, A. P.; Laaksonen, A.; Vorontsov-Velyaminov, P. N. *Mol. Phys.* **1994**, *82*, 455–471.
- (44) Sundholm, G.; Urbaniczky, C. Manuscript.
- (45) Lyubartsev, A. P.; Laaksonen, A.; Vorontsov-Velyaminov, P. N. *Mol. Simul.* **1996**, *18*, 43–58.
- (46) Lyubartsev, A. P.; Forrisdahl, O. K.; Laaksonen, A. *J. Chem. Phys.* **1998**, *108*, 227–233.
- (47) Wilding, N. B.; Muller, M. J. *J. Chem. Phys.* **1994**, *101*, 4324–4332.
- (48) Escobedo, F. A.; dePablo, J. J. *J. Chem. Phys.* **1995**, *103*, 2703–2710.
- (49) Errington, J. R.; Panagiotopoulos, A. Z. *J. Chem. Phys.* **1999**, *111*, 9731–9738.
- (50) Khare, A. A.; Rutledge, G. C. *J. Phys. Chem. B* **2000**, *104*, 3639–3644.

- (51) Boulougouris, G. C.; Errington, J. R.; Economou, I. G.; Panagiotopoulos, A. Z.; Theodorou, D. N. *J. Phys. Chem. B* **2000**, *104*, 4958–4963.
- (52) Toukan, K.; Rahman, A. *Phys. Rev. B* **1985**, *31*, 2643–2648.
- (53) Anderson, J.; Ullo, J. J.; Yip, S. *J. Chem. Phys.* **1987**, *87*, 1726–1732.
- (54) Mackerell, A. D.; et al. *J. Phys. Chem. B* **1998**, *102*, 3586–3616.
- (55) Frisch, M. J.; Trucks, G. W.; Schlegel, H. B.; Gill, P. M. W.; Johnson, B. G.; Robb, M. A.; Cheeseman, J. R.; Kieth, T.; Peterson, G. A.; Montgomery, J. A.; Raghavachari, K.; Al-Laham, M. A.; Zakrzewski, V. G.; Ortiz, J. V.; Foresman, J. B.; Cioslowski, J.; Stefanov, B. B.; Manaykkara, A.; Challacombe, M.; Peng, C. Y.; Ayala, P. Y.; Chen, W.; Wong, M. W.; Andres, J. L.; Repolage, E. S.; Gomperts, R.; Martin, R. L.; Fox, D. J.; Binkley, J. S.; Defrees, D. J.; Baker, J.; Stewart, J. P.; Head-Gordon, M.; Gonzales, C.; Pople, J. A.; *Gaussian 98*; Gaussian Inc.: Pittsburgh, PA, 1995.
- (56) Allen, M. P.; Tildesley, D. J. *Computer Simulations of Liquids*; Oxford: New York, 1987.
- (57) McCammon, J. A.; Harvey, S. C. *Dynamics of Proteins and Nucleic Acids*; Cambridge University Press: Cambridge, 1987.
- (58) Nöse, S. *Mol. Phys.* **1984**, *52*, 255–268.
- (59) Hoover, W. G. *Phys. Rev. A* **1985**, *31*, 1695–1703.
- (60) Tuckerman, M.; Berne, B. J.; Martyna, G. J. *J. Chem. Phys.* **1992**, *97*, 1990–2001.
- (61) Lyubartsev, A. P.; Laaksonen, A. *Comput. Phys. Commun.* **2000**, *128*, 565–589.
- (62) Hansmann, U. H. E. *Int. J. Mod. Phys. C* **1999**, *10*, 1521–1530.
- (63) Wong, M. W.; Frisch, M. J.; Wiberg, K. B. *J. Am. Chem. Soc.* **1991**, *113*, 4776.
- (64) Miertus, S.; Scrocco, E.; Tomasi, J. *Chem. Phys.* **1981**, *55*, 117.
- (65) Cieplak, P. *Pol. J. Chem.* **1998**, *72*, 1464–1471.